APPLIED PHYSICS LETTERS **86**, 1 (2005)

Photocurrent spectroscopy analysis of widely tunable negative-chirp quantum-well intermixed laser-modulator transmitters

G. B. Morrison[a)]
Department of Electrical and Computer Engineering, University of California–Santa Barbara, Santa Barbara, California 93106

J. W. Raring
Materials Department, University of California–Santa Barbara, Santa Barbara, California 93106

E. J. Skogen and C. S. Wang
Department of Electrical and Computer Engineering, University of California–Santa Barbara, Santa Barbara, California 93106

L. A. Coldren
Department of Electrical and Computer Engineering and Materials Department, University of California–Santa Barbara, Santa Barbara, California 93106

(Received 3 September 2004; accepted 20 December 2004)

High-speed laser-modulator transmitters fabricated using InGaAsP quantum-well intermixing exhibit negative chirp over a wavelength range of more than 30 nm. Photocurrent spectroscopy is used to examine the multiple band edges in these devices. An exciton peak is found in the photocurrent data, and the evolution of the band edge as a function of quantum-well intermixing and applied bias voltage is revealed. The photocurrent data are then exploited to verify and explain the negative chirp characteristics of the wavelength-agile transmitters. © *2005 American Institute of Physics*. [DOI: 10.1063/1.1865330]

Widely tunable laser-electro-absorption modulator (EAM) transmitters are ideal sources for next-generation optical networks. These monolithic wavelength-agile components promise cost savings in the form of inventory reduction, and are a key to technologies such as wavelength-routing and dynamic provisioning for future wavelength-division-multiplexing networks. Monolithic integration of separate laser and modulator band edges has been accomplished by numerous methods, but quantum-well intermixing (QWI) is an especially elegant approach, and is one of the simplest to implement.[1] QWI also allows simultaneous integration of passive waveguide sections, thereby reducing mirror loss. Using InGaAsP based QWI we have designed and fabricated widely tunable laser-EAMs that exhibit negative chirp and good extinction ratios over a wavelength range of more than 30 nm.[2] We attribute the excellent performance of the wavelength-agile modulator to the presence of a band edge exciton peak that is associated with the quantum confined stark effect (QCSE).[3] Quantum-well intermixing, however, is known to smooth out quantum well definition and to make the quantum wells broader and shallower,[4] altering, and potentially weakening or even extinguishing the exciton peak.[5] The degree of influence that QWI has on the QCSE in InGaAsP materials is not yet well established experimentally. In this letter, we use photocurrent spectroscopy to demonstrate that the QWI process can be exploited to obtain multiple band edges orthogonal to the growth direction while still retaining a strong exciton peak. The photocurrent data show the effect of QWI on the exciton peak in InGaAsP QW over a wide range of applied bias voltages. Furthermore, we model the large-signal chirp, starting with the photocurrent data, and demonstrate that the model is in good agreement with data collected from our widely tunable laser-EAM devices. The negative chirp of the widely tunable laser-EAM transmitter is thereby shown to be a direct result of the QWI band edge.

The laser-EAM transmitter device consists of a five-section sampled grating (SG) distributed Bragg reflector (DBR) laser, followed by an EAM. The five sections in the SGDBR, starting at the rear facet, are the back side absorber, the passive rear mirror, the passive phase section, the gain section, and a passive front mirror. The phase and mirror sections are used to tune the wavelength of the laser. The transmitter uses a buried ridge stripe architecture containing 15 InGaAsP 80 Å compressively strained (0.6%) quantum wells separated by 80 Å tensile-strained (0.3%) InGaAsP barriers. The quantum wells are centered within a 1.1Q waveguide that is 1.0 μm above an *n*-contact InGaAs layer that is grown on an Fe-doped InP substrate. Above the active region, a 15 nm InP regrowth layer, a 20 nm 1.3Q etch stop, and a 450 nm InP implant buffer layer were grown.

Gain and absorber sections of the transmitter were masked with 5000 Å of Si_xN_y and the wafer was exposed to a 5E14 cm^{-2} P^+ implant at 100 keV. The sample was then annealed at 675 °C until the desired band edge was obtained in the EAM sections. The photoluminescent peak (λ_{pl}) for the EAM QWI material was measured to be approximately 1510 nm. The implant layer in the EAM region was etched, and further annealing was performed on the wafer, causing the phase, mirror, and passive waveguide sections to shift to $\lambda_{pl} \approx 1450$ nm. The remaining implant layer was removed, stop etches were removed, and the wafer was submitted for metalorganic chemical vapor deposition (MOCVD) regrowth as described in Ref. 1. A more detailed description of the transmitter design and fabrication is available in Ref. 2. A schematic of the laser-modulator transmitter, and a cross-

[a)]Electronic mail: gmorrison@ece.ucsb.edu

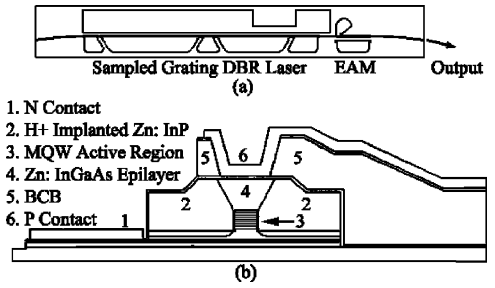

FIG. 1. (a) Diagram of the SGDBR laser module and electroabsorption modulator. (b) Cross-sectional schematic of the modulator component analyzed in this letter.

sectional view of the modulator, are shown in Figs. 1(a) and 1(b), respectively.

Identical material from the same MOCVD growth as was used for transmitter fabrication was simultaneously fabricated into circular photodiodes with radii ranging from 50 to 400 μm. These photodiodes were fabricated for the photocurrent spectroscopy characterization of the material. QWI was performed to obtain four different band edges for the photodiodes, with λ_{pl} at approximately 1554, 1527, 1508, and 1480 nm. The circular photodiode mesas were reactive-ion etched through the waveguide and quantum wells. The top InGaAs *p*-contact was thinner (750 Å) than on the transmitter devices in order to minimize absorption of input light. A 2000 Å layer of Si_xN_y was deposited, and circular vias were etched to expose the mesa contact layers. Ti/Pt/Au ring contacts and bonding pads were laid down and annealed at 420 °C for 30 s. A diagram of the basic structure of the photodiode is shown in Fig. 2.

Photodiodes were placed in a Varian Cary 500 spectrophotometer behind a 500 μm radius, position-adjustable aperture. The aperture served to sample a specific part of the spectrophotometer input beam, and input power was then easily calibrated using a Newport 1835 C optical power meter. A Kiethly 2400 L-V source meter was used to bias the photodiodes over a range of 0 to −6 V in −0.5 V increments. An EG&G lock-in Amplifier with a 1 s time constant was used in conjunction with a 3 kHz chopper to filter the photocurrent signal from leakage current and other noise. The entire system is automated. Reflectance and transmittance measurements on the spectrophotometer have been used to quantify the absorption of input light in the InGaAs *p*-contact material.

Photodiodes with 250 μm radii were found to be ideal candidates for easy alignment with the aperture, while coupling enough input light to generate a photocurrent signal well above the noise floor. A Ti/Pt/Au layer was deposited

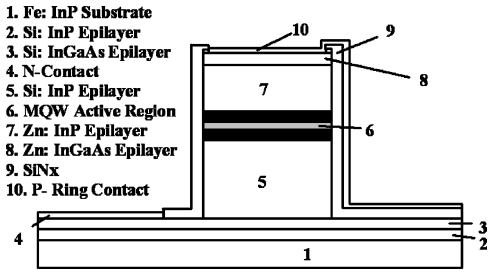

FIG. 2. Side view of the photodiode structure used for photocurrent spectroscopy.

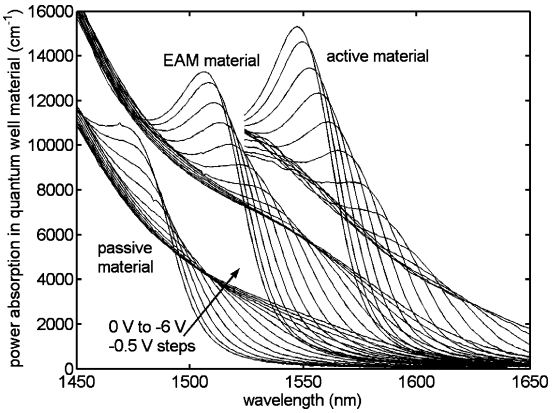

FIG. 3. Active, modulator, and passive absorption edges, obtained by ion-implant quantum-well intermixing. Curves are shown for biases ranging from 0 to −6 V in −0.5 V increments.

on the back side of the devices to prevent significant photocurrent contribution from backscattered light. Figure 3 shows the evolution of the band edge as a function of QWI and applied bias voltage. Band edges for as-grown material ($\lambda_{pl} \approx 1554$ nm), EAM material ($\lambda_{pl} \approx 1508$ nm), and passive material ($\lambda_{pl} \approx 1480$ nm) are shown. Note that the exciton peak for the QWI EAM material is strong, and that even the passive material exhibits an identifiable exciton peak. The carrier confinement in the quantum wells, however, is clearly reduced by QWI. The exciton is extinguished (i.e., electrons tunnel out of conduction band wells) at weaker biases when quantum-well intermixing is performed.

Starting with the absorption data for the EAM modulator in Fig. 3, differences in absorption between the band edge at 0 V and the band edges at each of the reverse biases are easily obtained. Application of the Kramers–Kronig transform, as described in Ref. 6, yields the index change as a function of voltage change. Although data in Fig. 3 are shown over a 200 nm range only, data spanning a full 280 nm was used for the truncated Kramers–Kronig transform. Figure 4 shows absorption changes ($\Delta\alpha$) and index changes (Δn) that are expected with −2 V change in potential, centered at bias voltages ranging from −1.5 to −5.0 V (e.g., a −2 V change in potential, centered at a bias voltage of −1.5 V, is from −0.5 to 2.5 V). With these −2 V changes, positive absorption changes ($\Delta\alpha$) are clearly seen throughout

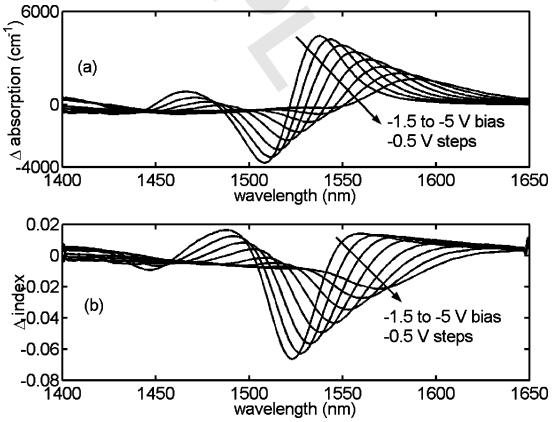

FIG. 4. (a) Changes in absorption with −2 V changes in potential that are centered at bias voltages ranging from −1.5 to −5 V. (b) Change in index with −2 V changes in potential that are centered at bias voltages ranging from −1.5 to −5 V.

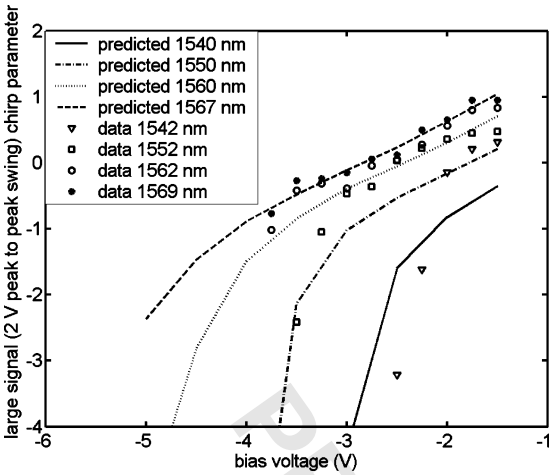

FIG. 5. Data points show measured chirp as a function of bias voltage at 1542, 1552, 1562, and 1569 nm. Lines show chirps predicted using photocurrent spectroscopy at 1540, 1550, 1560, and 1567 nm.

the operating range of the transmitter, as expected. At shorter wavelengths, in the vicinity of the exciton peak, negative absorption change ($\Delta\alpha$) occurs with a −2 V change in bias voltage. These trends directly influence the shape of the Δn curves [shown directly below Fig. 4(a) for comparison] by way of the Kramers–Kronig transform.

The $\Delta\alpha$ and Δn curves of Fig. 4 are in turn used to calculate the large-signal chirp.[7] Figure 5 compares the large-signal chirp, as calculated from photocurrent spectroscopy, at wavelengths of 1540, 1550, 1560, and 1567 nm, with the chirp measured in the buried-ridge modulators at wavelengths of 1542, 1552, 1562, and 1569 nm. The 2 nm differences between the wavelengths are included to account for the fact that the photocurrent diodes were intermixed to $\lambda_{pl} \approx 1508$ nm, whereas the transmitter EAMs were intermixed to $\lambda_{pl} \approx 1510$ nm. Chirp measurements were made on the transmitters using Agilent's Time Resolved Chirp software coupled with the required Agilent 86146B optical spectrum analyzer. The insertion loss of the modulator depends on the bias voltage and operating wavelength. For this device, a chirp of 0 can be obtained at all wavelengths in Fig. 5 (1542–1569 nm) with total insertion loss ranging from 3 to 4 dB, depending on the wavelength. Negative chirp of −0.7 can be obtained at all wavelengths in Fig. 5 with total insertion loss ranging from 3.5 to 9 dB, depending on the operating wavelength.[8]

In Fig. 5, the measured chirp parameter and the chirp parameter that is calculated directly from photocurrent spectroscopy are in reasonable agreement. There are no fitting parameters for the calculated curves. Clearly, the negative chirp performance of these wavelength-agile transmitters can be directly attributed to the QCSE band edge that is found in the QWI material from which the EAMs are fabricated. The QWI process that was used to shift the band edge in the EAM section of the device did not significantly detract from the exciton confinement. We therefore assert that QWI is a promising integration platform for implementation of high performance, widely tunable, negative chirp, laser-EAM transmitter devices.

In summary, quantum-well intermixing by ion implantation is a widely used technique for obtaining multiple band edges on a single wafer. We have presented detailed data examining the effect of QWI on InGaAsP quantum well band edges, over a wide range of bias voltages. We have used the data with the Kramers–Kronig transformation to experimentally verify that QWI laser-EAM transmitters can exhibit negative chirp over a range of 30 nm. The QWI process that was used to obtain the EAM band edge does not significantly detract from the exciton confinement, and thus the negative chirp exhibited by as-grown wells for a wide range of wavelengths is also exhibited in the QWI modulator wells. Quantum-well intermixing is therefore an excellent method for fabrication of integrated laser-EAM transmitters. We consider photocurrent spectroscopy to be an essential tool for understanding, designing, and analyzing complex QWI photonic integrated circuits.

[1]E. J. Skogen, J. W. Raring, J. S. Barton, S. P. Denbaars, and L. A. Coldren, IEEE J. Sel. Top. Quantum Electron. **9**, 1183 (2003).
[2]J. W. Raring, E. J. Skogen, L. A. Johansson, M. N. Sysak, J. S. Barton, M. L. Mašanovic, and L. A. Coldren, IEEE Photonics Technol. Lett. **16**, 1613 (2004).
[3]T. Yamanka, K. Wakita, and K. Yokoyama, Appl. Phys. Lett. **70**, 87 (1997).
[4]D. Hofstetter, B. Maisenhölder, and H. P. Zappe, IEEE J. Sel. Top. Quantum Electron. **4**, 794 (1998).
[5]E. H. Li and W. C. H. Choy, J. Appl. Phys. **82**, 3861 (1991).
[6]C. H. Henry, R. A. Logan, and K. A. Bertness, J. Appl. Phys. **52**, 4457 (1981).
[7]J. A. J. Fells, I. H. White, M. A. Gibbon, R. V. Penty, G. B. H. Thompson, A. P. Wright, R. A. Saunders, and C. J. Armistead, Electron. Lett. **30**, 2066 (1994).
[8]J. W. Raring, E. J. Skogen, S. P. DenBaars, and L. A. Coldren, Electron. Lett. (to be published).